

# A novel mutation of *LIM2* causes autosomal dominant membranous cataract in a Chinese family

Rui Pei<sup>1</sup>, Peng-Fei Liang<sup>2</sup>, Wei Ye<sup>1</sup>, Ji Li<sup>1</sup>, Ji-Yuan Ma<sup>1</sup>, Jian Zhou<sup>1</sup>

<sup>1</sup>Department of Ophthalmology, Xijing Hospital, Fourth Military Medical University, Xi'an 710032, Shaanxi Province, China

<sup>2</sup>Department of Otolaryngology, Xijing Hospital, Fourth Military Medical University, Xi'an 710032, Shaanxi Province, China

**Correspondence to:** Jian Zhou. Department of Ophthalmology, Xijing Hospital, Fourth Military Medical University, Xi'an 710032, Shaanxi Province, China. zhoujian@fmmu.edu.cn

Received: 2020-05-11 Accepted: 2020-07-02

## Abstract

• **AIM:** To identify mutations in the genes of a four-generation Chinese family with congenital membranous cataracts and investigate the morphologic changes and possible functional damage underlying the role of the mutant gene.

• **METHODS:** Whole exome analysis of thirteen members of a four-generation pedigree affected with congenital membranous cataracts was performed; co-segregation analysis of identified variants was validated by Sanger sequencing. All members underwent detailed physical and complete eye examinations. The physical changes caused by the mutation were analyzed in silico through homology modeling. The lens fiber block from a patient was observed under a scanning electron microscope (SEM). Cell membrane proteins and cytoplasmic proteins from the human lenses donated by one patient with cataract in this family and from the dislocated lens resulted from the penetrating ocular trauma of a patient unrelated with this family were extracted, and the expression and localization of MP20 and Cx46 were detected by Western blot (WB) assay in these proteins.

• **RESULTS:** A novel *LIM2* heterozygous mutation (c.388C>T, p.R130C) was identified with congenital membranous cataracts inherited by an autosomal dominant (AD) pattern. Nystagmus and amblyopia were observed in all patients of this family, and exotropia and long axial length were observed in most patients. A/B ultrasound scan and ultrasound biomicroscopy revealed obvious thin crystalline lenses from 1.7 to 2.7 mm in central thickness

in all cataract eyes. The bioinformatic analysis showed that the mutation was deleterious to the physiological function of *LIM2*-encoded MP20. Furthermore, by SEM, ultrastructure of the cataract nucleus showed that lens fiber cells (LFCs) remained morphologic characteristics of immature fiber cells, including flap cell surface with straight edges and lacking normal ball-and-socket joint boundaries, which implied that the differentiation of LFCs might be inhibited. Accumulation of MP20 and Cx46 in the cytoplasm was observed in the cytoplasm of the LFCs in human cataract lens.

• **CONCLUSION:** We identify a novel heterozygous *LIM2* (c.388C>T, p.R130C) mutation inherited by an AD pattern. This *LIM2* mutation causes the abnormal sub-localization of MP20 and Cx46 in LFCs resulting in membranous cataracts.

• **KEYWORDS:** *LIM2*; MP20; congenital cataract; missense mutation; differentiation

**DOI:**10.18240/ijo.2020.10.02

**Citation:** Pei R, Liang PF, Ye W, Li J, Ma JY, Zhou J. A novel mutation of *LIM2* causes autosomal dominant membranous cataract in a Chinese family. *Int J Ophthalmol* 2020;13(10):1512-1520

## INTRODUCTION

Congenital cataract is the second most common severe hereditary ocular disease in children, leading to serious visual impairments and even blindness<sup>[1]</sup>. Membranous cataract is a rarely reported category of congenital cataract. Its characteristic features include a prominent white mass at the center of the lens surrounding with a very small amount of lens cortex<sup>[2]</sup>. Few definite gene mutations have been reported which are associated with membranous cataracts without systematic diseases, one is a heterozygous c.465G>C mutation in exon 6 of *CRYBB2*, the other is a homozygous variant located in chromosome 1p34.3-p32.2 *via* linkage analysis<sup>[3-4]</sup>. Lens intrinsic membrane protein 2 (*LIM2*) gene encodes a conserved 173-amino acid (AA) integral membrane protein MP20 (alternatively known as MP17/MP18/MP19), which has a four-transmembrane topology and a W-GLW-C-C motif that defines the PMP-22/EMP/MP20/Claudin (Pfam00822) family of proteins<sup>[5-7]</sup> (Figure 1). Two mouse models related to the

*LIM2* mutation have been reported: one is To3 (total opacity of lens 3)<sup>[8]</sup>, a *LIM2* homozygous missense p.G15V mutation, and the other is an ENU (N-ethyl-N-nitrosourea)-generated mouse that is associated with a heterozygous c.151T>C (p.C51R) mutant. In addition, three mutations in *LIM2* and associated congenital cataracts have been reported: the homozygous mutation c.313T>C caused a p.F105V substitution in the third transmembrane domain of MP20, which is associated with pulverulent cortical and nuclear cataracts<sup>[9]</sup>, the homozygous c.587G>A (p.G154E) mutation disrupts the fourth transmembrane domain which is associated with juvenile-onset total cataracts<sup>[10]</sup>, and the homozygous c.233G>A (p.G78D) mutation in the second transmembrane domain of MP20 which is associated with the nuclear and subcapsular cataract<sup>[11]</sup> (Figure 1).

MP20 is exclusively expressed in lens fiber cells (LFCs) and is the second most prevalent membrane protein (MP) after MIP/AQP0 (major intrinsic protein/aquaporin-0)<sup>[5]</sup>. MP20 plays an important role in cell-cell adhesion and junction communication within avascular lens fibers<sup>[12-13]</sup>. MP20 displays different localization during LFC differentiation. In peripheral nucleated fiber cells, MP20 is in cytoplasm, while in deeper fiber cells, MP20 is at the plasma membrane<sup>[12,14]</sup>.

Connexin46 (Cx46) is a characteristically LFC-enriched gap junction protein, which colocalizes with MP20 in a restricted area, 0.5 to 1.0 mm into the lens from surficial cortex<sup>[15]</sup>. As one of the three connexin-family members (Cx43, Cx46, and Cx50)<sup>[16]</sup>, Cx46 is present only in LFCs throughout the outer 1 mm of the lens cortex, where its expression coincides with LFC differentiation<sup>[17]</sup>. During differentiation, Cx46 is mostly distributed in the plasma membrane and is highly expressed<sup>[18]</sup>. Therefore, the intracellular distribution of both MP20 and Cx46 could indicate the different stages of LFC differentiation indirectly.

In this study, we identified a novel mutation of *LIM2* that caused the changes on the second extracellular loop of MP20 and was associated with membranous cataracts. Interestingly, this mutation was characterized by an obvious thin crystalline lens in all cataract eyes, even in the 3-year-old patient within the family, which substantially differed from the three previously reported *LIM2* mutations<sup>[9-11]</sup>. Gatziofias *et al*<sup>[19]</sup> found that the normal differentiation process of lens epithelial cells (LECs) was disturbed *via* the histological examination of lens material from a membranous cataract. Thus, we suspected that the differentiation disturbance also occurred in this typical membranous cataract model. However, from the current literature on *LIM2* mutations causing congenital cataract and studies on the MP20 itself, we could not find any indication that *LIM2* mutations cause cataracts by affecting the differentiation of lens fibers.

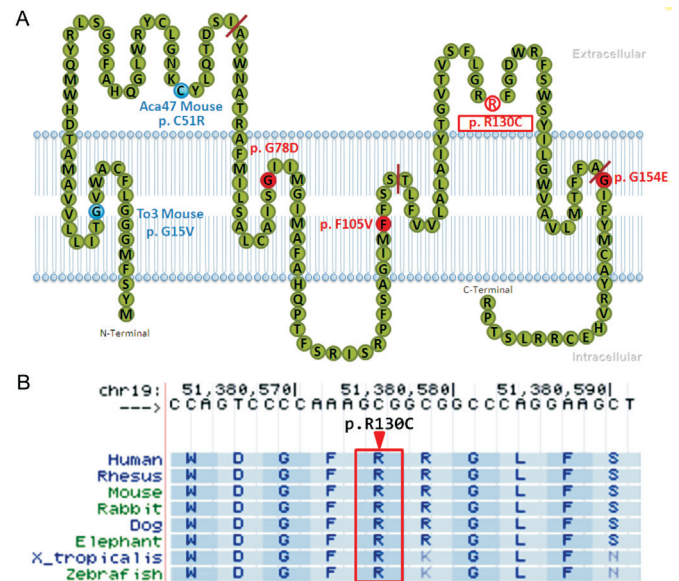


**Figure 1 MP20 and evolutionary conservation around the mutation site** A: Diagrammatic sketch of the AA composition of MP20. The four exon-encoded fragments are separated by short brown lines. Two mutated AAs in mouse models are labeled with a solid blue marker. Three mutated AAs previously reported in humans with congenital cataract are located on the second, third and fourth intracellular sections separately appear in solid red. The red box marks p.R130C on the second extracellular loop caused by the c.388C>T is discovered in our study. B: Evolutionary conservation of the altered AA residues among different biological species is shown in the red box (<http://genome.ucsc.edu/cgi-bin/hgTracks>).

In the present study, a novel *LIM2* (c.388C>T) heterozygous mutation in autosomal dominant (AD) inheritance pattern was identified from a four-generation Chinese family with membranous cataracts *via* whole-exome sequencing (WES). With scanning electron microscopy (SEM), a lens fiber block from a patient was observed to investigate the morphological characteristics of LFCs in cataract lens (CL). The human lenses specimens were employed to explore whether this *LIM2* mutation was associated with the differentiation process of LFC and the relationship between the genetic defect and the phenotype by evaluating the distribution of MP20 and Cx46 in cells.

**SUBJECTS AND METHODS**

**Ethical Approval** The Ethics Committee of the Fourth Military Medical University (Xi'an, China) approved this study on August 9<sup>th</sup>, 2017. The participants were recruited in July 2017, and the donor of the CL sample autonomously attended the hospital in November 2018. The clear lens was donated by a patient who had a penetrating injury, lens dislocation and a metal foreign body on the posterior wall of the eyeball in December 2019. All participants provided written informed consent prior to genetic testing and surgery per the tenets of the Declaration of Helsinki.

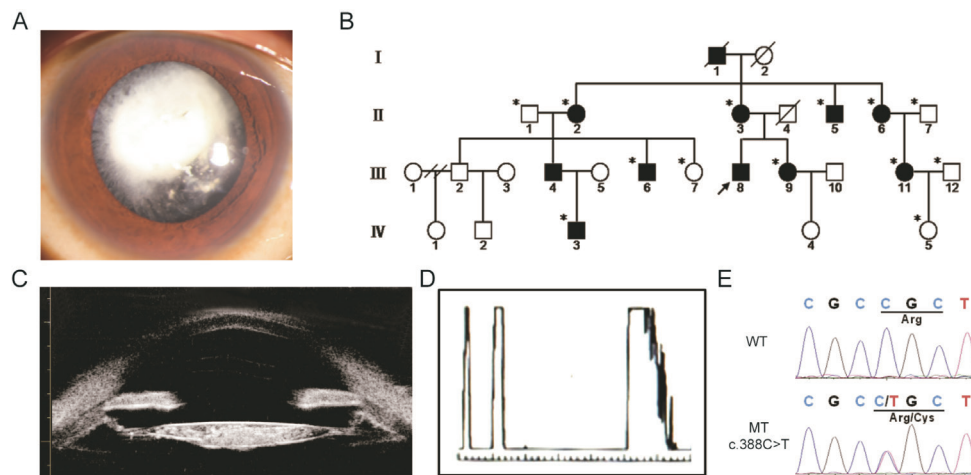


**Figure 2 Clinical characteristics and genomic analysis of the pedigree** A: Slit-lamp photograph of the right eye of III:8 depicts a membranous cataract with a dilated pupil; B: Pedigree of the four-generation family with congenital membranous cataracts. Squares and circles indicate males and females, respectively. Black symbols indicate affected individuals, and open symbols indicate unaffected individuals. The diagonal lines indicate deceased family members. Asterisks indicate family members who donated blood samples. The black arrow indicates the proband. C: UBM showed that the thickness of the lens became visibly thinner, especially in the peripheral cortical area. The iris position, lens diameter and suspensory ligament were unimpaired. D: A-ultrasonography showed that the lens thickness decreased to approximately 2.0 mm of the right eye of III:8; E: Comparison of the Sanger sequencing results of the unaffected (WT) and affected (MT) individuals. All affected individuals are heterozygous carriers. The *LIM2*: c.388C>T mutation results in the missense expression of MP20: p.R130C.

**Family and Preparation of Genomic DNA** A four-generation Chinese family with congenital membranous cataracts was recruited for clinical evaluation (Figure 2A). In addition to the proband, 13 participants donated blood samples, including eight affected and five unaffected individuals. In addition, another affected member of the family subsequently underwent small incision cataract surgery (SICS), and a lens sample was obtained from this individual. All family members had completed physical and eye examination, including visual acuity, slit-lamp biomicroscopy without and with dilation, and dilated fundus examinations. A/B-ultrasound scan, ultrasound biomicroscopy (UBM) and visual electrophysiology were also performed on all five cataract patients before cataract extraction.

Eight milliliters of peripheral blood were collected from each of 13 family members (Figure 2B). Genomic DNA was extracted from the blood samples using a QIAamp DNA blood midi kit (Qiagen, Hilden, Germany) according to the manufacturer's protocol.

**Target Exome Capture Sequencing and Bioinformatic Analysis** Polymerase chain reaction (PCR) and WES were performed on a HiSeq2000 sequencing platform (Illumina, San Diego, CA, USA) by the Annoroad Gene Technology (Co., Ltd., Beijing, China).

The target gene was identified that fulfilled the following criteria: 1) variants in the patients and normal in unaffected family members; 2) deny of missense, nonsense, frame shift, or splice site variants; nonsynonymous variants on coding

exonic portion; 3) absent or rare (frequency less than 1%) in three databases: Exome Aggregation Consortium (ExAC, <http://exac.broadinstitute.org>), 1000 Genomes (<http://www.internationalgenome.org>) and Exome Sequencing Project (ESP, <https://esp.gs.washington.edu/drupal>); and 4) predicted to be functionally deleterious based on mutation effect prediction tools (whole-exome SIFT, PolyPhen2 HDIV, PolyPhen2 HVAR scores from dbNSFP version 3.0a). Annotation was performed using ANNOVAR (v2017-06-01, Wang Genomics Lab, Los Angeles, USA).

**Validation of Mutations and Segregation Analysis** Specific primer pairs were designed to amplify regions harboring point mutations using the Primerblast Tool (<https://www.ncbi.nlm.nih.gov/tools/primer-blast>). PCR and Sanger sequencing were applied to validate whether the candidate *LIM2* mutation was present in all patients and absent in all unaffected individuals among the 13 familial participants (forward primer: 5'-CAGAGACAATGGCCAATTAC-3'; reverse primer: 5'-GAGCCCAACACCCTACTCTC-3').

Furthermore, DNA extracted from 100 blood samples from unrelated control individuals was subjected to PCR and Sanger analysis using the same primers (Qingke Bio, Xian, China) in the same manner to validate that the mutation is absent in unaffected individuals.

Finally, sequencing data were compared with reference sequences in the NCBI GenBank using Chromas software (v2.1.3, Technelysium Pty. Ltd., Australia) and the reported mutations in the literature to ensure the novelty of the mutation.

**Digital 3-dimensional Structure Rebuilding and Functional Prediction** Homologous model structures of wild type (WT) and mutant type (MT) MP20 were predicted with the Swiss-Model program (<https://www.swissmodel.expasy.org>) based on the WT (NP\_001155220.1, [https://www.ncbi.nlm.nih.gov/protein/NP\\_001155220.1](https://www.ncbi.nlm.nih.gov/protein/NP_001155220.1)) and mutant MP20 sequences were retrieved from ModBase (<https://modbase.compbio.ucsf.edu/modbase-cgi/index.cgi>). The spatial conformation and the changes in covalent bonds around the mutant AA were analyzed by Swiss-PdbViewer (v3.7, GlaxoSmithKline R&D, UK)<sup>[20-21]</sup>.

The hydropathicity, hydrophobicity, polarity values and average flexibility of MP20 in WT and MT were compared using ProtScale on the ExPASy Server (<http://www.expasy.org/tools/protscale.html>).

#### **Preparation of Scanning Electron Microscopy Specimen**

The central part of the lens tissue (residual fiber block) of the right eye of patient III:4 was collected during SICS and immediately fixed in a mixture of 2% paraformaldehyde and 2.5% glutaraldehyde in 0.1 mol/L sodium cacodylate buffer for 24h<sup>[22]</sup>. Then, the block was divided in half and fixed for another 24h. After dehydration using acetone and critical point drying, both halves were split into quarters, yielding fresh fracture surfaces. The specimens were sputter coated with gold powder and examined under SEM (S-3400N, HITACHI, Japan).

**Western Blot Analysis** The total protein (TP), MP and cytoplasmic protein (CP) of control clear lens (Con) and CL were extracted respectively using a membrane and cytoplasmic protein extraction kit (Keygen Biotech, Nanjing, China). The proteins were quantitated using a BCA Protein Assay kit (Beyotime, Shanghai, China) according to the manufacturer's instructions. The proteins were separated by SDS-PAGE electrophoresis with 8% acrylamide and transferred to 0.45  $\mu$ m polyvinylidene fluoride (PVDF) membranes. The membranes were then incubated with rabbit anti-MP20 polyclonal antibody (1:500, PA5-43463, Thermo Fisher, Waltham, USA), mouse anti-Cx46 monoclonal antibody (1:1000, sc-365394, Santa Cruz Biotechnology, Santa Cruz, USA), mouse anti-GAPDH IgG monoclonal antibody (1:1000, ab8245, Abcam, Cambridge, UK) and rabbit anti-ATP1A1 (ATPase, Na/K transporting, alpha 1 polypeptide) polyclonal antibody (1:1000, T02901, Proteintech, Chicago, USA), followed by horseradish peroxidase goat anti-rabbit/mouse IgG (1:3000, Jackson ImmunoResearch, USA). Enhanced chemiluminescence (Thermo Fisher Scientific, Rockford, USA) was used to visualize the protein bands. Finally, all bands were scanned and analyzed. The expression levels of proteins in TP and CP were normalized with GAPDH, and proteins in MP were normalized with Na/K ATPase.

**Statistical Analysis** All numerical data were shown as the mean $\pm$ standard deviation (SD). Two-tailed unpaired Student's *t*-test was used for comparison between two samples.

#### **RESULTS**

**Clinical Evaluation** Based on the presence of affected individuals in each of the four generations, and the cosegregation with the heterozygous variants, AD inheritance of the congenital membranous cataracts was demonstrated. In total, there were 11 affected individuals (cataract patients) and 15 unaffected members within the pedigree (Figure 2B), without consanguineous marriages. Their cataracts were bilateral and in the same phenotype from the youngest 3-year-old IV:3 to the oldest 59-year-old II:2. The age of onset was the early infant stage according to inquiries into the family history. Visual acuity ranged from light perception (LP) to 20/63 in the unoperated cataract individuals. Nystagmus and amblyopia were observed in all patients, and exotropia was revealed in eight of 11 patients. Under a slit-lamp biomicroscope, through a dilated pupil, we detected a thin white lens nucleus, fibrotic anterior lens capsule with calcified spots, and a tiny cortex in the peripheral part of the lens, which were typical characteristics of membranous cataracts (Figure 2A). UBM and an A-ultrasound scan revealed obvious thin lenses from 1.7 to 2.7 mm in all cataract individuals (Figure 2C, 2D). The axial length was elongated in most patients, and the average length was 24.46 mm (Table 1).

Within the family, nine eyes from five patients (III:4, III:6, III:8, III:9, IV:3), including the proband, underwent cataract extraction and IOL implantation surgeries at Xijing Hospital by the same surgeon. The best corrected visual acuity (BCVA) for these patients was improved from 20/800 to 20/125 at three months after surgeries. There was no other family history of ocular diseases or systemic abnormalities.

**Mutational Assessment and Validation Analysis** WES was performed to identify the putative pathogenic mutation using peripheral blood genomic DNA from the affected and unaffected members of the pedigree. After the removal of sequencing adapters and low-quality bases, approximately 12.53 GB of clean sequencing data were obtained for each sample. More than 99.50% of the sequencing reads were aligned to the human reference genome, and at least 75.54% effective reads from target regions were collected after the removal of PCR duplications. The average sequencing depth for each sample was 95-106-fold, with more than 93.68% target regions on average exhibiting at least a 10-fold coverage. After the exclusion of frequent variants and the application of technical and biological filters, a database including 82 525 single nucleotide polymorphisms (SNP), 10 864 insertion-deletions (InDel) and 135 structural variations (SV) was established. Though the cosegregation of genotypes and

## A novel *LIM2* mutation causes membranous cataract

**Table 1 The clinical features of all participants in the Chinese family**

Family member	Gender	Age (y)	UCVA (R; L)	Axial length (mm)	Lens thickness (mm)	Nystagmus	Strabismus	Lens R/L
II:1	M	56	20/20; 20/20			N	N	Clear
II:2	F	59	20/100; 20/63			Y	N	Membranous
II:3	F	54	LP; LP			Y	Exotropia	Membranous
II:5	M	51	20/667; 20/800			Y	Exotropia	IOL/IOL
II:6	F	49	CF/30 cm; HM/20 cm			Y	Exotropia	Membranous
II:7	M	50	20/25; 20/20			N	N	Clear
III:4	M	31	20/160; 20/200	25.20/25.50	2.6/2.7	Y	Exotropia	Membranous
III:6	M	23	20/500; HM/20 cm	22.74/24.64	1.7/2.0	Y	Exotropia	Membranous
III:7	F	25	20/20; 20/20			N	N	Clear
III:8	M	31	20/160; 20/400	24.10/24.50	2.0/2.3	Y	Exotropia	Membranous
III:9	F	29	20/160; 20/400	27.00/26.67	IOL/1.9	Y	Exotropia	IOL/membranous
III:11	F	26	20/63; 20/50			N	N	Membranous
III:12	M	27	20/12.5; 20/12.5			N	N	Clear
IV:3	M	6	20/800; 20/250	22.09/22.19	2.2/2.1	Y	Exotropia	Membranous
IV:5	F	3	20/40; 20/50			N	N	Clear

N: No; Y: Yes.

**Table 2 Annotated variants by WES analysis in 13 participants**

Gene	Chromosome position	Nucleotide change	Amino acid change	Novelty	Mutation taster	SIFT	Polyphen2 HDIV	1000G	ExAC	Genotype
OR2T8	chr1:248084464	c.145T>C	p.Trp49Arg	rs11204564	P	0.297/T	0/B	.	0.7463	Homozygous
FAT2	chr5:150930186	c.4543G>A	p.Gly1515Ser	rs2278370	P	0.192/T	0.012/B	0.116014	0.0983	Heterozygous
FAT2	chr5:150930345	c.4384G>A	p.Val1462Met	rs2278371	P	0.121/T	0.034/B	0.122404	0.1	Heterozygous
ETFB	chr19:51857738	c.155C>T	p.Pro52Leu	rs79338777	P	0/D	0.001/B	0.0772764	0.0739	Heterozygous
SIGLEC10	chr19:51919217	c.785G>A	p.Arg262His	rs141425782	N	0.282/T	0.748/P	0.0047923	0.002	Heterozygous
LIM2	chr19:51883831	c.388C>T	p.Arg130Cys	Novel	D	0.001/D	1/D	.	.	Heterozygous
FPR1	chr19:52249809	c.439A>T	p.Ile147Phe	rs183314714	N	0.242/T	0.001/B	0.0011981	0.0003	Heterozygous
LAMA5	chr20:60899182	c.5722G>A	p.Ala1908Thr	rs11698080	P	0.497/T	0.002/B	0.215056	0.2266	Homozygous

phenotypes was done for each variant, total 39 SNPs and 3 InDels were annotated. In these variants, there were only 8 nonsynonymous SNPs on coding exonic portion after the deletion of nonsense, frame shift, and splice site variants (Table 2). Three of 8 SNPs had a frequency less than 1%, and then their functional impairments were assessed based on mutation effect prediction tools. Finally, only the mutation of *LIM2* was predicted to be functionally deleterious, based on the Polyphen2 (Polymorphism Phenotyping v2) HDIV and HVAR score of the mutation was one, and the SIFT score was 0.001, which predicted its damage to the function of MP20. Thus, we identified a novel *LIM2* mutation c.388C>T (Chromosome 19q13.41, GenBank accession number, NM\_001161748.1) in exon 4, which caused a p.R130C change at the second extracellular loop of MP20.

We have registered this novel mutation of *LIM2* in ClinVar with the variation accession number VCV000625113.1 in April 2019, and it could be retrieved in The Single Nucleotide

Polymorphism Database (dbSNP) and 1000 Genomes Project (1000G) with ID rs15684800549.

Sanger sequencing validation analysis was applied to verify the heterozygous mutation in the 13 participants of this family and 100 unrelated individuals without cataracts. Compared with the unaffected family members and the 100 unrelated normal controls, the mutation cosegregated with the cataract phenotype of all diseased individuals, and all phenotypes manifested as heterozygous (Figure 2E).

### Three-dimensional Homologous Structural Models and Bioinformatic Analysis

We examined WT-MP20 and MT-MP20 on the homologous model structures and chemical characteristics by the Swiss-Model program. Both spatial structures of the whole protein and the second extracellular loop were not altered obviously (Figure 3A), but the covalent bonds around the variant AA changed drastically. When the Arg was replaced by Cys, an additional new hydrogen bond formed between 130Cys and 128Gly, which may alter the

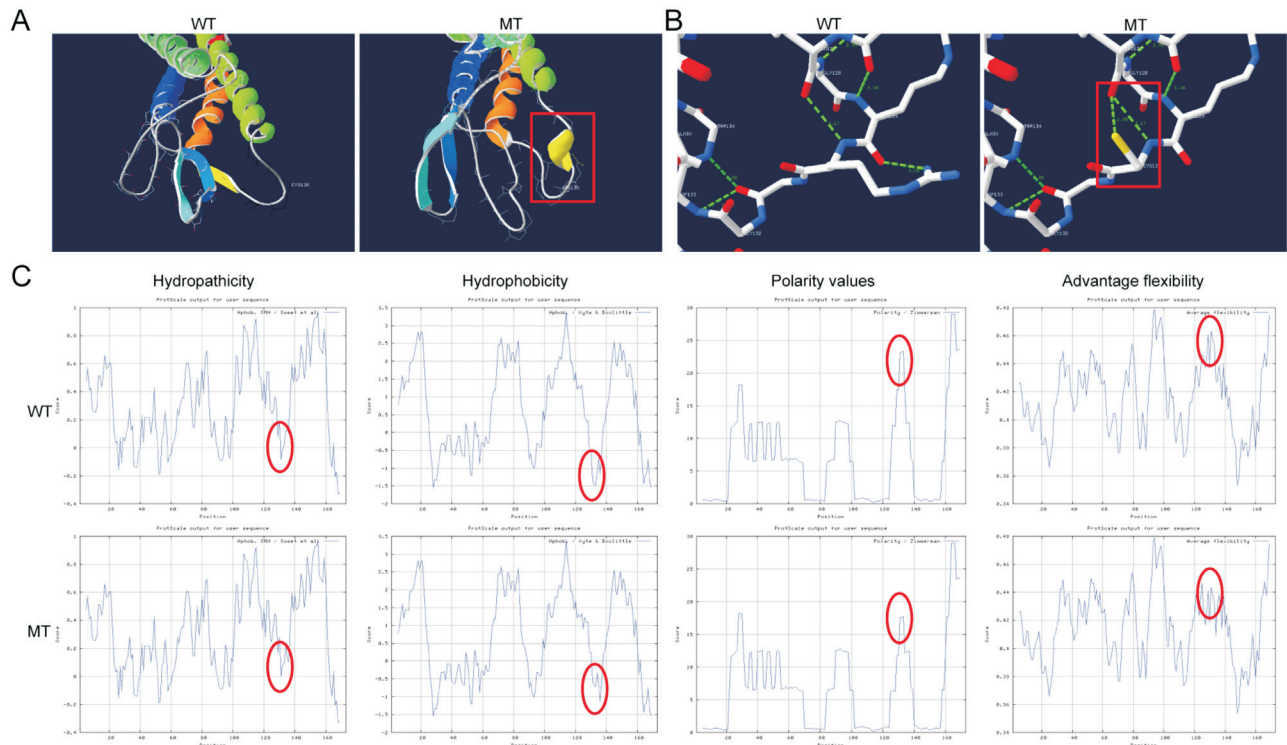


**Figure 3 Digital 3-dimensional structure and function prediction** A: Homologous model structures predicted by the Swiss-Model program. An alpha helix structure on the second extracellular loop of MP20 formed after the mutation. B: Chemical characteristics of WT MP20 and MT MP20. An additional hydrogen bond was established between 130Cys and 128Gly in mutant MP20 due to the reactive sulfhydryl group labeled as a yellow rod. C: Compared with the WT MP20, mutant MP20 potentially exhibits higher hydropathicity and hydrophobicity indicated by the red ellipse in the first and second rows. In addition, lower polarity values and average flexibility are indicated in the third and fourth rows with the red ellipse. The y-axis represents the values of hydropathicity, hydrophobicity, polarity and average flexibility in eight individual graphics.

topological structure of the protein because of the medium strength of the newly formed hydrogen bond (Figure 3B).

ProtScale software predicted that the MT-MP20 would have higher hydrophobicity, lower polarity values and lower average flexibility compared with the WT-MP20 (Figure 3C).

#### Ultrastructural Analysis by Scanning Electron Microscopy

The peripheral surrounding bulk cortex exhibited numerous vacuoles and structural breakdown issues. However, some residual and stop-in-sudden fiber “shelf” could be slightly recognized in the outer zone of the lens nucleus (Figure 4D). Widespread fusion was noted between LFCs, which exhibited a lichenoid-like flap cell surface in the center of the lens bulk (Figure 4E).

Two types of interdigitating joint populations, such as fingerlike structures and reciprocal pits<sup>[23]</sup>, presented on the long flat surface of the hexagonal fibers and in the adjacent fibers in normal lens (Figure 4A), but in the cataract specimen these structures were totally changed. Instead of the normal wavy fingerprint pattern (Figure 4D), a dense lichenoid-like pattern was present on the CL fibers. A few finger-like joints covered by lichenoid structure were scattered on the flap surface. Massive cracks were present along the cell-to-cell junctions (Figure 4E). A few narrow cells surrounded by

lichenoid-like structures were detected in the nuclear of CL (Figure 4F).

#### The Expression Levels of MP20 and Cx46 by Western Blot Analysis

In human CL, MP20 expression was stronger in cytoplasm and lower in membrane than that in the control lens, respectively. There were apparently differences between the CL and control lens on the distribution of Cx46 in cytoplasm and membrane, which was similar with that in MP20 (Figure 5). Since the lack of sufficient number of affected and control lens specimens, we could only repeat the Western blot (WB) experiments of two specimens three times, so the data could not be compared statistically.

#### DISCUSSION

In this study, we have investigated the genetic defects of membranous cataracts inherited by AD in a four-generation Chinese family associated with *LIM2* mutation of the c.388C>T, resulting in the changes of the second extracellular loop of MP20. Morphological changes of the cataract were characterized by thin lens under bio-microscope, and immature fiber cells in the lens nucleus and a massive breakdown of the cortex under SEM.

The novel *LIM2* mutation (c.388C>T) is very different from all reported mutations of *LIM2*, which is the first heterozygous

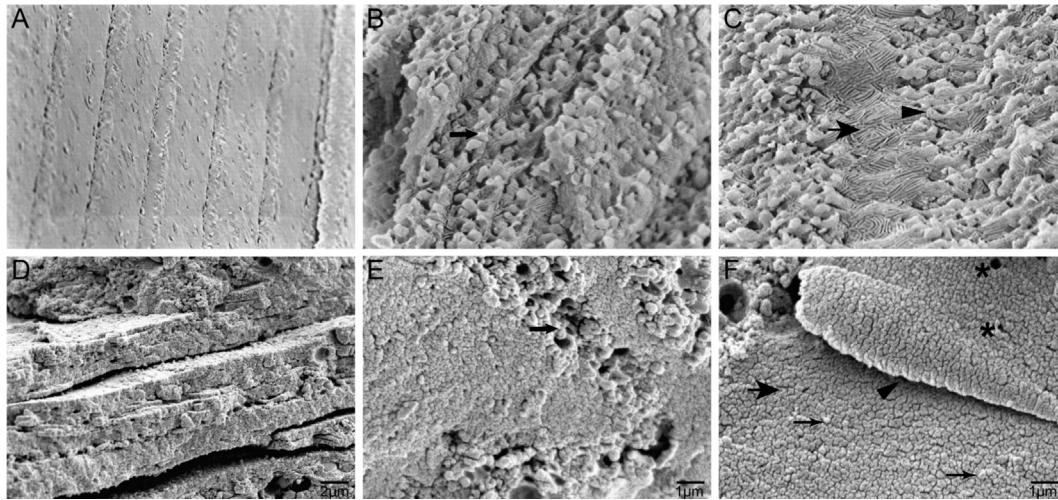


**Figure 4** The morphological differences between the normal human lens and the lens of the patient with the mutation (Figure 4A-4C were produced by Stirling and Griffiths<sup>[23]</sup>) A: The cortex of normal human lens exhibited regular fiber arrangement. B: The joints on the junctions between normal fibers in the deepest cortical and most superficial nuclear regions and ball-and-socket joints (arrow) are predominant between the lateral sides of the LFCs. C: Furrowed membranes with the fingerprint pattern (spear point) are prominent surface characteristics of embryonic nucleus fibers, and the ball-and-socket joints are still present in fiber junctions (arrowhead). D: The cortex of the lens of the patient with the mutation. The fiber “shelf” was broken down and only minimally recognized. E: The junctions of the lens nucleus of mutated patient exhibit a lower depth of bites and distribution density of the ball-and-sockets. In addition, massive cracks were present among the ball-and-socket joints, as noted by the arrow. F: Widespread fusion was noted between LFC membranes that exhibited a widespread “lichenoid” (spear point) flap surface, and the edge of the fiber cell was straight and oblong (arrowhead) in the lens nucleus of the mutated patient. Random fingerlike (narrow arrow) and hole (asterisk) segments were scattered on the flap surface with a lichenoid overcoat.

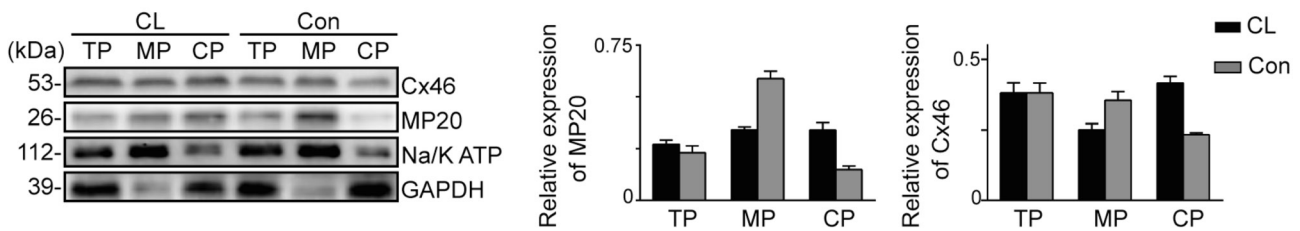


**Figure 5** WB analysis of MP20 and Cx46 in TP, MP and CP of control and CL.

mutation of *LIM2* causing cataracts identified in human family and inherited by the AD pattern, since the reported three mutations in *LIM2* were all homozygous and related to AR congenital cataracts in humans.

As for the other potential harmful heterozygous mutation of *LIM2* c.67A>C identified from an age-related cortical cataract patients, the inheritance mode was not clear<sup>[24]</sup>. This novel *LIM2* mutation resulting in the change on the second extracellular loop of MP20 is the first mutation site on this loop to be found so far. The phenotype of cataract in this family is not only different from the other *LIM2* mutations' but also implies that this *LIM2* mutation causes some fatal functional changes in LFCs. Because there is no intermarriage between family members in this pedigree, which is different from the reported three families, this mutation may increase the harmful impact factor.

Based on the bioinformatic analysis, the mutation may draw a Cys into the second extracellular loop of MP20, generates

a new moderate-strength hydrogen bond with a nearby AA and an extra dystopia disulfide bond around the mutation site, which could form a reactive sulfhydryl group in the side chain of Cys. This reactive group could be oxidized and then form a new more stable disulfide bond with other Cys, resulting in an alteration in the function of native MP20 by disrupting membrane-associated topology<sup>[25]</sup>.

The morphological changes of lens fibers vary from the superficial cortex to the center of the lens under SEM, representing the differentiation stage of fiber cells<sup>[26-27]</sup>. In the nucleus of the lens, the normal fetal and embryonic fiber cells were polygonal with many sides, and the ball-and-socket joints predominated at the junctions of the long and short sides. This cataract specimen was the center of the lens, but the cells did not exhibit the appearance of the mature fiber cells. There were mainly two differences. Firstly, the residual cells exhibited wide and flap appearance, and lacked any normal boundaries between cells. Straight and oblique cell edges in these cells

indicated they were characterized by immature cortical fibers. Secondly, the texture of the two types of interacting joints between the cataract and normal specimens were different. A few finger-like structures were observed on the flap surface of the fiber cells of cataract, which supposedly been observed on the normal immature cortical fiber membranes<sup>[23]</sup>. However, the fingerprint processes, which was predominated the normal lens fiber flap surface, were replaced by lichenoid-like appearance. Native furrowed appearance and regular spatial arrangement were lost as well. Therefore, in addition to the devastating breakdown of the lens fiber tissue, an extensive amount of immature fibers was present in the inner core, and these fibers contributed to the formation of cataracts in the mutant lens and served as an underlying obstacle to the differentiation of mutant LFCs.

It has been found that the insertion of MP20 into LFC membranes plays a critical role in lens transparency<sup>[28]</sup>. In our study, MP20 is markedly accumulated in the LFC cytoplasm of CLs by WB assays, suggesting that this mutation leads to abnormal localization of MP20 in the LFCs thus results in cataracts. Simultaneously, the *LIM2* mutation in To3 mice results in severe damage to LFCs in the lens core and nuclear cataract, and in cell lines expressing the To3 mutation, MP20 fails to insert into the plasma membrane<sup>[14,29]</sup>. Subsequently, Chen *et al*<sup>[30]</sup> reported that the first 25 AAs of MP20 was sufficient to target and apparently integrate the protein into the cell membrane. However, the c.388C>T mutation resulted in a change in the AA at position 130 of MP20, but the distribution on the cell membrane of MP20 was still blocked, which differed from the previous conclusions.

As a distinct protein of LFC, MP20 displays different localization during LFC differentiation: in peripheral nucleated fiber cells (primary fibers), MP20 is in cytoplasm, while in deeper fiber cells (secondary/mature fiber), MP20 is on the plasma membrane<sup>[12,14]</sup>. The marked accumulation of MP20 in the LFC cytoplasm of CLs was similar to the characteristic distribution of LECs. So, we speculate that this mutation may prevent the differentiation of LFCs and result in LFCs maintaining more LECs' characteristics from the point of abnormal distribution of MP20.

To test our hypothesis further, we employ Connexin46 that is characteristically enriched in LFCs. It has been reported that Cx46 is in large plaques on the broad faces of the LFCs throughout the outer 1 mm of the lens cortex, and MP20 is co-localized in a restricted area 0.5 to 1.0 mm into the lens, in which LFCs are still at primary differentiation stage<sup>[15]</sup>. In the LFC cytoplasm of CLs, the localization of Cx46 in the cells is similar to that of MP20 and highly expressed, which is consistent with the results of Tenbroek *et al*<sup>[15]</sup>. Furthermore, the expression of Cx46 coincides with fiber cell differentiation<sup>[17]</sup>.

During differentiation, most Cx46 in cytoplasm inserts into the plasma membrane and is highly expressed<sup>[18]</sup>. Therefore, accumulation of Cx46 in the cytoplasm in the cytoplasm of CLs may suggest that the differentiation of LFCs is disturbed by this mutation.

In summary, the identification of *LIM2* mutation (c.388C>T) related membranous cataracts should be a starting point to broaden the recognition of the function of the second extracellular loop of MP20, adding a new dimension to the understanding of its protein function during differentiation and suggesting a new potential pathogenesis of membranous cataracts.

#### ACKNOWLEDGEMENTS

We would like to thank the family members and blood sample donors for their cooperation and participation. We also extend our thanks to the patient who kindly agreed to donate a sample of lens cortex from a traumatic cataract.

**Foundations:** Supported by the National Natural Science Foundation of China (No.81370998); Department of Science and Technology of Shaanxi Province (No.2019JM-065).

**Conflicts of Interest:** Pei R, None; Liang PF, None; Ye W, None; Li J, None; Ma JY, None; Zhou J, None.

#### REFERENCES

- 1 Gilbert C, Foster A. Childhood blindness in the context of VISION 2020—the right to sight. *Bull World Heal Organ* 2001;79(3):227-232.
- 2 Messina-Baas O, Cuevas-Covarrubias SA. Inherited congenital cataract: a guide to suspect the genetic etiology in the cataract genesis. *Mol Syndromol* 2017;8(2):58-78.
- 3 Chen WR, Chen XY, Hu ZM, Lin HT, Zhou FQ, Luo LX, Zhang XY, Zhong XJ, Yang Y, Wu CR, Lin ZL, Ye SB, Liu YZ. A missense mutation in CRYBB2 leads to progressive congenital membranous cataract by impacting the solubility and function of  $\beta$ B2-crystallin. *PLoS One* 2013;8(11):e81290.
- 4 Butt T, Yao WL, Kaul H, Xiaodong J, Gradstein L, Zhang Y, Husnain T, Riazuddin S, Hejtmancik JF, Riazuddin SA. Localization of autosomal recessive congenital cataracts in consanguineous Pakistani families to a new locus on chromosome 1p. *Mol Vis* 2007;13:1635-1640.
- 5 Arneson ML, Louis CF. Structural arrangement of lens fiber cell plasma membrane protein MP20. *Exp Eye Res* 1998;66(4):495-509.
- 6 Taylor V, Welcher AA, Program AE, Suter U. Epithelial membrane protein-1, peripheral myelin protein 22, and lens membrane protein 20 define a novel gene family. *J Biol Chem* 1995;270(48):28824-28833.
- 7 Gehne N, Haseloff R, Blasig I. Identity crisis in the PMP-22/EMP/MP20/Claudin superfamily (Pfam00822). *Tissue Barriers* 2015;3(4):e1089680.
- 8 Steele EC, Wang JH, Lo WK, Saperstein DA, Li X, Church RL. *Lim2*(To3) transgenic mice establish a causative relationship between the mutation identified in the *lim2* gene and cataractogenesis in the To3 mouse mutant. *Mol Vis* 2000;6:85-94.

- 9 Pras E, Levy-Nissenbaum E, Bakhan T, Lahat H, Assia E, Geffen-Carmi N, Frydman M, Goldman B, Pras E. A missense mutation in the LIM2 gene is associated with autosomal recessive presenile cataract in an inbred Iraqi Jewish family. *Am J Hum Genet* 2002;70(5):1363-1367.
- 10 Ponnampalagan SPG, Ramesha K, Tejwani S, Matalia J, Kannabiran C. A missense mutation in LIM2 causes autosomal recessive congenital cataract. *Mol Vis* 2008;14:1204-1208.
- 11 Irum B, Khan SY, Ali M, Kaul H, Kabir F, Rauf B, Fatima F, Nadeem R, Khan AO, Al Obaisi S, Naeem MA, Nasir IA, Khan SN, Husnain T, Riazuddin S, Akram J, Eghrari AO, Riazuddin SA. Mutation in LIM2 is responsible for autosomal recessive congenital cataracts. *PLoS One* 2016;11(11):e0162620.
- 12 Gonen T, Grey AC, Jacobs MD, Donaldson PJ, Kistler J. MP20, the second most abundant lens membrane protein and member of the tetraspanin superfamily, joins the list of ligands of galectin-3. *BMC Cell Biol* 2001;2(1):1-12.
- 13 Gutierrez DB, Garland DL, Schwacke JH, Hachey DL, Sehey KL. Spatial distributions of phosphorylated membrane proteins aquaporin 0 and MP20 across young and aged human lenses. *Exp Eye Res* 2016;149:59-65.
- 14 Grey AC, Jacobs MD, Gonen T, Kistler J, Donaldson PJ. Insertion of MP20 into lens fibre cell plasma membranes correlates with the formation of an extracellular diffusion barrier. *Exp Eye Res* 2003;77(5):567-574.
- 15 Tenbroek E, Arneson M, Jarvis L, Louis C. The distribution of the fiber cell intrinsic membrane proteins MP20 and connexin46 in the bovine lens. *J Cell Sci* 1992;103 ( Pt 1):245-257.
- 16 Beyer EC, Kistler J, Paul DL, Goodenough DA. Antisera directed against connexin43 peptides react with a 43-kD protein localized to gap junctions in myocardium and other tissues. *J Cell Biol* 1989;108(2):595-605.
- 17 Paul DL, Ebihara L, Takemoto LJ, Swenson KI, Goodenough DA. Connexin46, a novel lens gap junction protein, induces voltage-gated currents in nonjunctional plasma membrane of *Xenopus* oocytes. *J Cell Biol* 1991;115(4):1077-1089.
- 18 Rong P, Wang X, Niesman I, Wu Y, Benedetti LE, Dunia I, Levy E, Gong XH. Disruption of Gja8 (alpha8 connexin) in mice leads to microphthalmia associated with retardation of lens growth and lens fiber maturation. *Dev Camb Engl* 2002;129(1):167-174.
- 19 Gatziofufas Z, Huchzermeyer CR, Hasenfus A, El-Husseiny M, Seitz B. Histological and biochemical findings in membranous cataract. *Ophthalmic Res* 2012;47(3):146-149.
- 20 Arnold K, Bordoli L, Kopp J, Schwede T. The SWISS-MODEL workspace: a web-based environment for protein structure homology modelling. *Bioinformatics* 2006;22(2):195-201.
- 21 Guex N, Peitsch MC. SWISS-MODEL and the Swiss-Pdb Viewer: an environment for comparative protein modeling. *Electrophoresis* 1997;18(15):2714-2723.
- 22 Blankenship T, Bradshaw L, Shibata B, Fitzgerald P. Structural specializations emerging late in mouse lens fiber cell differentiation. *Invest Ophthalmol Vis Sci* 2007;48(7):3269-3276.
- 23 Stirling RJ, Griffiths PG. Scanning EM studies of normal human lens fibres and fibres from nuclear cataracts. *Eye (Lond)* 1991;5(1):86.
- 24 Zhou Z, Wang BB, Hu SS, Zhang CM, Ma X, Qi YH. Genetic variations in GJA3, GJA8, LIM2, and age-related cataract in the Chinese population: a mutation screening study. *Mol Vis* 2011;17:621-626.
- 25 Wedemeyer WJ, Welker E, Narayan M, Scheraga HA. Disulfide bonds and protein folding. *Biochemistry* 2000;39(15):4207-4216.
- 26 Taylor VL, Al-Ghoul KJ, Lane CW, Davis VA, Kuszak JR, Costello MJ. Morphology of the normal human lens. *Investig Ophthalmol Vis Sci* 1996;37(7):1396-1410.
- 27 Zampighi GA, Hall JE, Ehring GR, Simon SA. The structural organization and protein composition of lens fiber junctions. *J Cell Biol* 1989;108(6):2255-2275.
- 28 Steele EC, Kerscher S, Lyon MF, Glenister PH, Favor J, Wang J, Church RL. Identification of a mutation in the MP19 gene, Lim2, in the cataractous mouse mutant To3. *Mol Vis* 1997;3:5.
- 29 Shiels A, King JM, MacKay DS, Bassnett S. Refractive defects and cataracts in mice lacking lens intrinsic membrane protein-2. *Investig Ophthalmol Vis Sci* 2007;48(2):500-508.
- 30 Chen T, Li XL, Yang Y, Erdene AG, Church RL. Does lens intrinsic membrane protein MP19 contain a membrane-targeting signal? *Mol Vis* 2003;9:735-746.